EBioMedicine 15 (2017) 90–99

Contents lists available at ScienceDirect

EBioMedicine

journal homepage: www.ebiomedicine.com

Research Paper

Oncogenic KRas-induced Increase in Fluid-phase Endocytosis is Dependent on N-WASP and is Required for the Formation of Pancreatic Preneoplastic Lesions

Clara Lubeseder-Martellato [a,*], Katharina Alexandrow [a], Ana Hidalgo-Sastre [a], Irina Heid [b], Sophie Luise Boos [a,c], Thomas Briel [a], Roland M. Schmid [a,c], Jens T. Siveke [a,c,d,**]

[a] Clinic and Polyclinic for Internal Medicine II, Klinikum Rechts der Isar, Technical University of Munich, Germany
[b] Institute of Radiology, Klinikum Rechts der Isar, Technical University of Munich, Germany
[c] German Cancer Consortium (DKTK) and German Cancer Research Center, DKFZ, Heidelberg, Germany
[d] Division of Solid Tumor Translational Oncology, German Cancer Consortium (DKTK), Partner Site Essen, West German Cancer Center, University Hospital Essen, Germany

ARTICLE INFO

Article history:
Received 15 July 2016
Received in revised form 28 November 2016
Accepted 20 December 2016
Available online 24 December 2016

Keywords:
Oncogenic KRas
Fluid-phase endocytosis
Pancreatic ductal adenocarcinoma (PDAC)
Acinar-to-ductal metaplasia (ADM)
Acinar epithelial explants
Neural-Wiskott-Aldrich syndrome protein (N-WASP)
Mice models

ABSTRACT

Fluid-phase endocytosis is a homeostatic process with an unknown role in tumor initiation. The driver mutation in pancreatic ductal adenocarcinoma (PDAC) is constitutively active $KRas^{G12D}$, which induces neoplastic transformation of acinar cells through acinar-to-ductal metaplasia (ADM). We have previously shown that $KRas^{G12D}$-induced ADM is dependent on RAC1 and EGF receptor (EGFR) by a not fully clarified mechanism. Using three-dimensional mouse and human acinar tissue cultures and genetically engineered mouse models, we provide evidence that (i) $KRas^{G12D}$ leads to EGFR-dependent sustained fluid-phase endocytosis (FPE) during acinar metaplasia; (ii) variations in plasma membrane tension increase FPE and lead to ADM *in vitro* independently of EGFR; and (iii) that RAC1 regulates ADM formation partially through actin-dependent regulation of FPE. In addition, mice with a pancreas-specific deletion of the Neural-Wiskott–Aldrich syndrome protein (N-WASP), a regulator of F-actin, have reduced FPE and impaired ADM emphasizing the *in vivo* relevance of our findings. This work defines a new role of FPE as a tumor initiating mechanism.

1. Introduction

In normal cells, KRas is activated by upstream tyrosine kinases, including EGFR, for further downstream signaling through the RAF-MEK-ERK cascade. However, in several human cancers, mutated KRas is constitutively active and does not require upstream activation, thus fulfilling one of the hallmarks of cancer cells (Hanahan and Weinberg, 2011). $Kras^{G12D}$ is the driving oncogenic mutation of pancreatic ductal adenocarcinoma (PDAC), one if not the most fatal human cancers (Almoguera et al., 1988). PDAC develops through preneoplastic lesions originating from acinar-to-ductal metaplasia (ADM) (Aichler et al., 2012; Means et al., 2005). Despite being constitutively active, $KRas^{G12D}$ requires upregulated expression of the tyrosine kinase EGF receptor (EGFR) for ADM development (Ardito et al., 2012; Navas et al., 2012) and its downstream target *Rac1* for correct actin organization (Heid et al., 2011; Means et al., 2005). However, how oncogenic KRas and EGFR cooperate for ADM development remains still unclear.

EGFR requires ligand binding for activation, activated EGFR signals from the plasma membrane to downstream targets and is subsequently internalized through endocytosis (Fehrenbacher et al., 2009; Oda et al., 2005; Warren and Landgraf, 2006). Endocytosis controls cellular homeostasis, is tightly regulated and involves several mechanisms that can be both receptor-driven and receptor-independent. Fluid-phase endocytosis (FPE) includes endocytic pathways that have fluid phase markers as cargos (Doherty and McMahon, 2009; Grant and Donaldson, 2009; Stenmark, 2009). Recent work supports a regulatory role of endocytosis in the net signaling output of malignant cells (Joffre et al., 2011; Mosesson et al., 2008; Murphy et al., 2009; Scita and Di Fiore, 2010; Sorkin and von Zastrow, 2009). However, the impact of an endocytic mechanism, in particular of FPE, in the early development of preneoplastic transformation in the pancreas has not been defined yet.

Here, we show that sustained FPE is required for the development of ADM. Our data indicate that oncogenic $KRas^{G12D}$ in acinar cells leads to an EGFR-dependent increase in FPE to drive the formation of precancerous lesions and that an increase in FPE can lead to ADM independently

* Corresponding author.
** Corresponding author at: Division of Solid Tumor Translational Oncology, West German Cancer Center, University Hospital Essen, Germany.
E-mail addresses: clara.lubeseder-martellato@tum.de (C. Lubeseder-Martellato), j.siveke@dkfz.de (J.T. Siveke).

http://dx.doi.org/10.1016/j.ebiom.2016.12.013

of EGFR expression. We also provide *in vivo* evidence that the KRas-induced increase in FPE is dependent on N-WASP expression. Thus, our data provide a new link between oncogenic KRas and sustained FPE during pancreatic cancer initiation.

2. Materials and Methods

Ptf1a$^{Cre/wt}$, *Kras*$^{LSL\text{-}G12D/wt}$, *Egfr*$^{\Delta/\Delta}$, $^{\Delta/\Delta}$, *N-Wasp*$^{\Delta/\Delta}$ and *p53*$^{\Delta/\Delta}$ strains have previously been described (Ardito et al., 2012; Heid et al., 2011; Hingorani et al., 2003; Lommel et al., 2001). Experiments were conducted in accordance with the German Federal Animal Protection Laws and were approved by the Institutional Animal Care and Use Committees of the Technical University of Munich.

2.2. Human Samples

This study conformed to the Declaration of Helsinki and was approved by the ethics committee of the Technical University of Munich. Informed consent was obtained from all patients included in the study (project number 365/13). Human acinar epithelial explants were isolated from the normal tissue surrounding surgically resected human PDAC.

2.3. Acinar Epithelial Explants

Pancreatic epithelial explants were prepared as described in (Lubeseder-Martellato, 2013). Recombinant mouse EGF (R&D Systems; final concentration, 25 ng/ml) was added when indicated. Compounds were added once to the media the same day of isolation (defined as day 1). Wortmannin, cytochalasin D (Sigma), monensin (Calbiochem) and refametinib (Selleckchem) were used. For ADM quantification, acinar explants were seeded at least in triplicates and ADM was quantified from 3 to 8 optical fields per well by counting rounded acinar-cell clusters and flat duct-like cell clusters lining a hole. Quantification of ADM was confirmed by immunofluorescence or western blot analysis for CK19 expression in the ductal structures.

2.4. Fluid-phase Endocytosis (FPE) Assays

Two methods described in the supplementary information (SI) were used as a functional assay for the quantification of receptor-independent endocytosis. All FPE assays were performed one day after isolation of acinar explants if not other specified.

2.5. Immunoisolation

RAB5 + endosomes were isolated using MACS technology. See the SI section.

2.6. Immunohistochemistry and Immunofluorescence

Standard staining techniques were used. See the SI section.

2.7. Western Blots

Standard western blotting was used. For a list of antibodies used see the SI section.

2.8. Statistics

Statistical analyses were performed using unpaired, two-tailed student's *t*-test or Mann–Whitney test. In all box plots the central line is the median of the data and the whiskers represent maximum and minimum values.

3. Results

3.1. FPE Is Increased in Oncogenic KRas-mediated Preneoplastic Development

PDAC patients have mutated KRas in about 95% of the cases (Hruban et al., 2001). Using cBioBiortal (Cerami et al., 2012; Gao et al., 2013) we found that up to 10% of genes involved in the endolysosomal system were upregulated in PDAC patients (Fig. 1A and Supplementary Table 1). When the tumors were dichotomized for alterations in these genes, patients with respective alterations had a significantly reduced survival (Fig. S1A).

Human and mouse PDAC can originate from pancreatic acinar cells through acinar-to-ductal metaplasia (ADM) (Aichler et al., 2012; Means et al., 2005). Conditional *Ptf1a*$^{Cre/wt}$;*Kras*$^{LSL\text{-}G12D/wt}$ mice (*Kras*^{G12D}) develop ADM within few weeks postnatally (Fig. S1B). RAB5 is the rate-limiting component of the endocytic machinery, thus we next analyzed expression of RAB5. RAB5 was strongly expressed in ADM lesions in *Kras*^{G12D} mice (Fig. 1B), and both RAB5 and active RAB5-GTP increased in pancreatic whole tissue lysates of *Kras*^{G12D} mice with age (Fig. S1E). To further analyze endocytic pathways during ADM, we used primary acinar epithelial explants from *Kras*^{G12D} mice (termed *Kras*^{G12D} explants), which developed ADM *in vitro* within 3 days and upregulated EGFR expression when cultivated in 3D-collagen matrix (Fig. S1B-D). Similarly, wild type explants develop ADM when treated with EGF (Fig. S1F) (Ardito et al., 2012). Notably, both *Kras*^{G12D} and wild type explants can be inhibited by the allosteric MEK1/2 inhibitor refametinib as previously shown (Ardito et al., 2012; Iverson et al., 2009) (Fig. S1F). Thus, both *Kras*^{G12D} and EGF-treated wild type acinar explants mimic ADM and depend on activation of the EGFR-MEK-ERK pathway, providing a model to further investigate the molecular mechanisms underlying ADM.

As for murine explants, acinar explants from human pancreatic tissue developed ADM *in vitro* within few days (Fig. 1C,D) in agreement with previous studies (Eser et al., 2013). We next analyzed the uptake of fluid-phase markers, which increased as ADM progressed both in human (Fig. 1E) and in mouse explants (Figs. 1F, S1G). Notably, this applied both for *Kras*^{G12D}- and EGF- driven ADM. This result was supported by the observation that the number of vesicles positive for EEA1 increased from day 1 to day 3 during ADM in *Kras*^{G12D} explants (Fig. S1H-I), while neither total EEA1 nor total RAB5 expression increased in *Kras*^{G12D} explants (not shown). Next, we investigated if oncogenic *KRas* could influence FPE levels in mouse acinar cells. FPE was significantly increased in freshly isolated *Kras*^{G12D} explants compared to controls (Fig. 1G). To confirm this result *in vivo*, we measured dextran uptake in 4 weeks old mice; at this age, acini from wild type and *Kras*^{G12D} mice were morphologically indistinguishable and both express the acinar marker amylase (Fig. 1H). FPE was significantly increased in the pancreata of *Kras*^{G12D} mice (Fig. 1I). A further type of endocytosis called macropinocytosis is upregulated in oncogenic *Kras*^{G12D} transformed cells (Commisso et al., 2013), however FPE levels were unaffected in a panel of human pancreatic cell lines with or without oncogenic *KRas* mutation (Fig. S1J). Thus, fluid-phase endocytosis is induced by oncogenic KRas in acinar cells before development of ADM *in vivo* and is not regulated by oncogenic *KRas* once cells are transformed.

3.2. FPE increases while ADM Occurs and is EGFR-dependent

We next took advantage of the compounds monensin and wortmannin that affect the endolysosomal system among other effects. Monensin increases pH in intracellular organelles, inhibits receptor recycling and perturbs the endomembrane system. Wortmannin perturbs endocytosis by inhibition of phosphoinositide 3-kinase (Li et al., 1995; Stein et al., 1984). First, we used the two compounds to assess whether they can be used to inhibit FPE in acinar explants; both compounds reduced FPE (Fig. 2A). Second, we looked at the effect of the

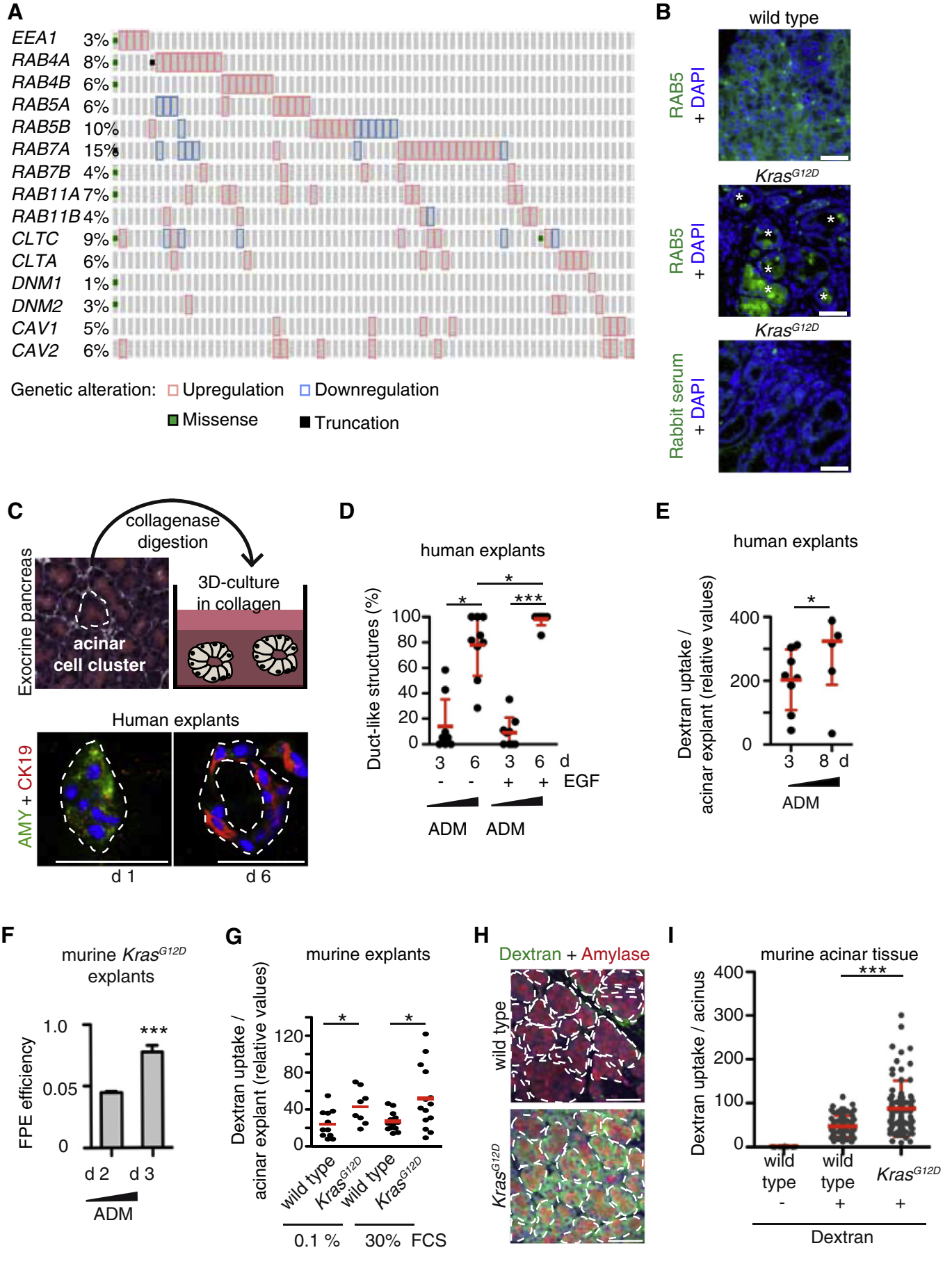
A
EEA1 3%
RAB4A 8%
RAB4B 6%
RAB5A 6%
RAB5B 10%
RAB7A 15%
RAB7B 4%
RAB11A 7%
RAB11B 4%
CLTC 9%
CLTA 6%
DNM1 1%
DNM2 3%
CAV1 5%
CAV2 6%
Genetic alteration: Upregulation Downregulation Missense Truncation
B
wild type
RAB5 + DAPI
KrasG12D
RAB5 + DAPI
KrasG12D
Rabbit serum + DAPI
C
collagenase digestion
Exocrine pancreas
acinar cell cluster
3D-culture in collagen
Human explants
AMY + CK19
d 1
d 6
D
human explants
Duct-like structures (%)
3 6 3 6 d
- - + + EGF
ADM ADM
E
human explants
Dextran uptake / acinar explant (relative values)
3 8 d
ADM
F
murine KrasG12D explants
FPE efficiency
d 2 d 3
ADM
G
murine explants
Dextran uptake / acinar explant (relative values)
wild type KrasG12D wild type KrasG12D
0.1 % 30% FCS
H
Dextran + Amylase
wild type
KrasG12D
I
murine acinar tissue
Dextran uptake / acinus
wild type - wild type + KrasG12D +
Dextran

two compounds on ADM; both drugs inhibited ADM *in vitro* after 3 days of culture in a dose-dependent manner and were not toxic (Figs. 2B-C, S2C). P-ERK was reduced upon pharmacological treatment and was still low at day 3 (Figs. 2D, S2B). Similar results were obtained for EGF-treated wild type explants (Fig. S2A, D–E) inhibitors affect FPE in acinar explants through perturbation of the Golgi apparatus, which is intimately connected to the endomembrane-system. Although the inhibitory effect of these compounds on ADM may be due to their actions on other pathways such as PI3K, these data suggest a potential involvement of FPE in acinar-to-ductal metaplasia that was further elucidated as described below.

Since reduction of P-ERK may be responsible for the blockade of ADM, we further analyzed the pancreatic cancer cell lines Capan1 and BxPc3. Here, monensin reduced FPE rates but increased P-ERK (Fig. S2F–G). This result supports a direct drug effect on FPE, while down regulation of P-ERK may be secondary in acinar cells but not in fully transformed cancer cells.

We next investigated pathways potentially involved in the regulation of fluid-phase endocytosis during ADM. Activation of P-ERK occurs during both KRas and EGF-mediated ADM. Thus, we investigated whether P-ERK is required for the increase in FPE levels by using the MEK inhibitor refametinib that inhibited P-ERK activation in acinar explants (Fig. 2E). Refametinib did not affect FPE levels (Fig. 2F). We conclude that the increase of FPE does not require P-ERK activation in this context. Endocytosis is regulated by various mechanisms and some of them involve actin and the small GTPase RAC1 (Doherty and McMahon, 2009). Moreover, we have previously shown that RAC1-dependent actin polymerization is required for ADM in a mouse model with conditional deletion of *Rac1* (*Rac1*$^{\Delta/\Delta}$) (Heid et al., 2011). Thus, we hypothesized a link between RAC1-regulated actin polymerization and the increase in fluid-phase endocytosis and used a pharmacological and genetic approach to test this hypothesis. We could block the increase of FPE upon EGF treatment in acinar explants both by pharmacological inhibition of actin polymerization with cytochalasin D (CytD) and by genetic depletion of *Rac1* using *Rac1*$^{\Delta/\Delta}$ mice (Fig. 2G-H). In agreement with these results, FPE was reduced also by genetic depletion of *Rac1* in a *Kras*^{G12D} background using acinar explants from *Rac1*$^{\Delta/\Delta}$;*Kras*^{G12D} mice (Fig. 2I). Hence, the increase of the fluid-phase endocytosis rates relies on RAC1-dependent actin polymerization during ADM.

In the canonical EGFR signaling pathway, activation of EGFR is required for KRas downstream signaling. Both constitutive active KRas^{G12D} and EGFR activation lead to ADM. However, genetic concomitant activation of oncogenic KRas and loss of EGFR in murine pancreas (*Kras*^{G12D};*Egfr*$^{\Delta/\Delta}$) impairs ADM development (Ardito et al., 2012). Since the amount of EEA1-positive vesicles increased in *Kras*^{G12D} but not *Kras*^{G12D};*Egfr*$^{\Delta/\Delta}$ explants with time (Fig. S1I), we next analyzed FPE using a functional dextran uptake assay performed on freshly isolated acinar explants. We found that explants lacking EGFR had reduced FPE rates (Fig. 2J–K). We conclude that oncogenic KRas requires EGFR for sustained fluid-phase endocytosis.

3.3. Variations in Plasma Membrane Tension Increase FPE and Induce ADM independently of EGFR

We next aimed to address the role of EGFR-independent FPE. Variations in plasma membrane tension caused by changes in osmolarity modulate endocytosis (Apodaca, 2002). Since *Kras*^{G12D};*Egfr*$^{\Delta/\Delta}$ mice do not develop tumors (Ardito et al., 2012) and thus no PDAC cell lines could be established from this model, we used *Kras*^{G12D};*p53*$^{\Delta/\Delta}$;*Egfr*$^{\Delta/\Delta}$ mice to isolate and culture primary tumor cells with active oncogenic KRas lacking EGFR, and used these cells for stable expression of EGFR (Fig. S3A). Treatment with hypoosmolar medium increased FPE in all cell lines, thus this method is suitable to induce FPE in a receptor-independent manner (Fig. S3B–C). We next applied hypoosmolar medium to wild type explants. Here, FPE increased and induced ADM (Fig. 3A-B) in concomitance to activation of P-ERK and P-AKT (Figs. 3C, S3D). CytD inhibited both FPE and ADM in this setting and was not toxic as evaluated by LDH-assay (Fig. S3E–G). Thus, hypoosmotic stress-induced ADM is characterized by similar features as EGF-induced ADM.

Since *Kras*^{G12D};*Egfr*$^{\Delta/\Delta}$ explants do not develop ADM *in vitro* under our standard conditions (Fig. 3D) (Ardito et al., 2012), we next treated them with hypoosmolar medium, which increased endocytosis (Fig. 3E) and induced a partial rescue of the ADM phenotype (Fig. 3F–G) and P-ERK activation that persisted at day 3 (Fig. 3H). P-ERK activation was observed also in *Kras*^{G12D} explants after hypoosmotic treatment (Fig. 3H). Similarly, hypoosmolar medium partially induced ADM *in vitro* in *Egfr*$^{\Delta/\Delta}$ explants (Fig. S3H). In a second experimental approach, a mechanical strain was applied, since this may affect endocytosis (Apodaca, 2002). Mechanical strain slightly increased FPE and induced duct-like structures and P-ERK activation in *Kras*^{G12D};*Egfr*$^{\Delta/\Delta}$ explants (Fig. S4A–D). In summary, a receptor-independent increase of FPE is sufficient to overcome the requirement of EGFR for the development of duct-like structures and ERK phosphorylation in a three-dimensional explant model for acino-ductal metaplasia.

To gain further molecular insights, we analyzed ADM lesions by confocal imaging. We observed a partial overlap of ERK1 with RAB5 (Fig. 3I). We next immunoisolated the RAB5+ fraction from pancreatic tissue of wild type and *Kras*^{G12D} mice. EEA1 was detected in the RAB5+ fraction (magnetic fraction, MF), while the plasma membrane marker E-cadherin (CDH1) was absent, confirming successful isolation of the early endosomal fraction (Fig. 3J). Part of total ERK was found in the MF fraction of *Kras*^{G12D} pancreata only (Fig. 3K), in agreement with the confocal data. We next performed a mass spectrometry analysis of the RAB5+ fraction of *Kras*^{G12D} pancreatic tissue to identify proteins bound to early endosomes. Here, IQGAP1 was found in the top 8 hits present in the high molecular weight fraction (Supplementary Table 2). RAB5 interacts with IQGAP1, which is a scaffold protein that modulates ERK activation (Jacquemet and Humphries, 2013; Jameson et al., 2013). Accordingly, IQGAP1 was found in the MF of *Kras*^{G12D} pancreatic tissue together with RAB5 (Fig. S4E). Thus, one possible mechanism may be a scaffold function of early endosomes together with IQGAP1 for sustained ERK activation to drive ADM.

Fig. 1. FPE is increased in oncogenic KRas-mediated preneoplastic development. (A) Genetic alterations in genes involved in the endolysosomal system in human PDAC samples (TGCA provisional, $N = 145$ patients). (B) Pancreata from mice of the indicated genotypes were analyzed by immunofluorescence. A rabbit *anti*-RAB5 antibody was used. Normal rabbit serum was used as matched negative control. Images were taken with the same exposition time for each slide. The bright green dots seen in each panel are erythrocytes. Asterisks highlight preneoplastic lesions expressing high RAB5 levels. Scale bars = 50 μM. (C) Top: schematic representation of acinar cell explants. Bottom: immunofluorescence staining of human acinar explants for the acinar cell marker amylase and the ductal marker cytokeratin 19 (CK19). (D) Quantification of ADM using human explants in collagen matrix. Each dot represents the number of structures/optical field. Red lines: mean ± SD. Mann-Whitney test. (E) A dextran uptake assay was performed using human acinar explants. The graph shows quantification of the dextran uptake per single acinar explant. Red lines: mean ± SD. Mann-Whitney test. (F) HRP uptake endocytic assay in *Kras*^{G12D} acinar explants at the indicated time points. Mean ± SD. Two-tailed *t*-test. (G) Acinar explants were starved overnight and then a dextran uptake assay was performed. Each dot represents the uptake in one single acinar explant; red lines: mean ± SD; Mann-Whitney test. (H) Lysine-fixable dextran was injected i.v. in 4 weeks-old mice of the indicated genotypes. After 15 min, mice were sacrificed and perfused. Representative total *Z*-stack projections of immunofluorescence staining for dextran and amylase are shown. Dashed lines highlight the acini in the tissue. (I) Quantification of (H). Endocytic efficiency was quantified per amylase-positive acini. Red lines: mean ± SD; Mann-Whitney test. All scale bars = 50 μm.

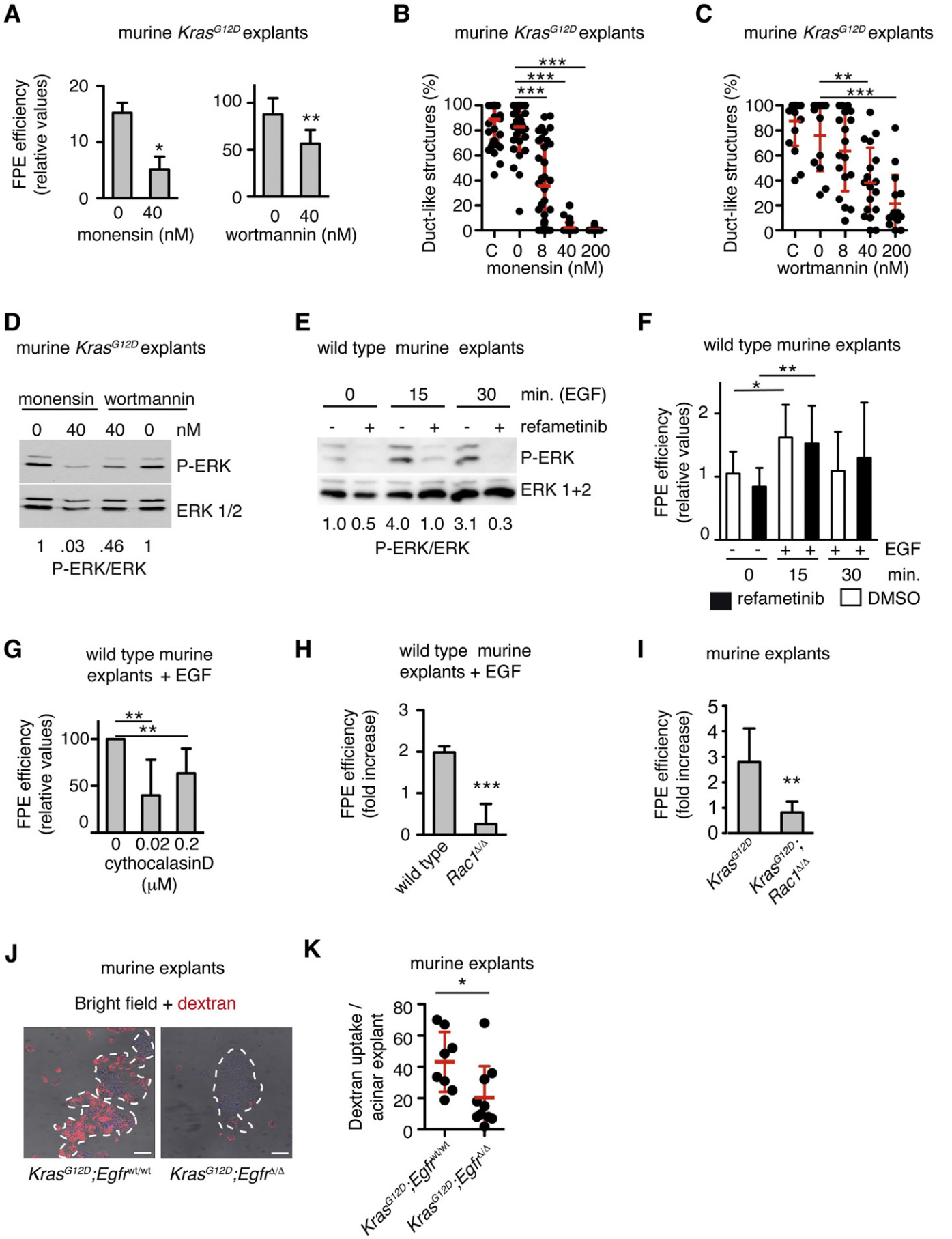
A
murine KrasG12D explants
FPE efficiency (relative values)
monensin (nM)
wortmannin (nM)
B
murine KrasG12D explants
Duct-like structures (%)
monensin (nM)
C
murine KrasG12D explants
Duct-like structures (%)
wortmannin (nM)
D
murine KrasG12D explants
monensin wortmannin
nM
P-ERK
ERK 1/2
P-ERK/ERK
E
wild type murine explants
min. (EGF)
refametinib
P-ERK
ERK 1+2
P-ERK/ERK
F
wild type murine explants
FPE efficiency (relative values)
EGF
min.
refametinib
DMSO
G
wild type murine explants + EGF
FPE efficiency (relative values)
cythocalasinD (μM)
H
wild type murine explants + EGF
FPE efficiency (fold increase)
wild type
Rac1Δ/Δ
I
murine explants
FPE efficiency (fold increase)
KrasG12D
KrasG12D; Rac1Δ/Δ
J
murine explants
Bright field + dextran
KrasG12D;EgfrWt/wt
KrasG12D;EgfrΔ/Δ
K
murine explants
Dextran uptake / acinar explant
KrasG12D;EgfrWt/wt
KrasG12D;EgfrΔ/Δ

3.4. Sustained FPE Precedes ERK Activation Following Hypoosmotic Treatment

In order to investigate whether an increase in FPE is important for MEK/ERK activation, we looked for the effect of MEK inhibition on the hypoosmolar medium-induced ADM. *Kras*^{G12D} acinar explants were isolated and treated with hypoosmolar medium for five minutes to induce FPE (Figs. S4F and 4A). The MEK inhibitor refametinib was added immediately after the hypoosmotic treatment (Fig. S4F). Refametinib did not reduce the amount of FPE (Fig. 4A), which is in line with the results obtained with the EGF-induced FPE (Fig. 2F). In contrast, refametinib inhibited hypoosmotic stress-induced ADM *in vitro* (Figs. 4B-C and S4G). Thus, hypoosmotic stress-induced ADM is dependent of MEK/ERK activation like EGF- and *Kras*^{G12D}-dependent ADM. These results also indicate that most likely an increase of FPE precedes MEK/ERK activation.

3.5. Oncogenic-Kras-driven Preneoplastic Development Relies on N-Wasp

IQGAP1 interacts, among many other proteins, with N-WASP (the homolog of human *WASL*), an actin nucleation factor that regulates EGFR internalization and degradation (Takenawa and Miki, 2001; Benesch et al., 2005). In PDAC patients, *EGFR* and *WASL* mRNA expression correlated each other and with the expression of early endosomal genes *EEA1* and *RAB5A* but not with the late endosomal genes *RAB7* and *RAB9* (Fig. 5A). In *Kras*^{G12D} mice, we found expression of N-WASP in precursor lesions as well as in PDAC (Figs. 5B, S5A), while N-WASP was absent in *Kras*^{G12D}*;Egfr*$^{\Delta/\Delta}$ pancreata (Fig. 5C). These data suggest a link between N-WASP, the endosomal compartment and tumor initiation. Thus, we generated mice with conditional pancreas-specific deletion of *N-Wasp* with and without concomitant activation of oncogenic *Kras*^{G12D}.

N-Wasp$^{\Delta/\Delta}$ and *Kras*^{G12D}*;N-Wasp*$^{\Delta/\Delta}$ mice were viable and born at Mendelian ratio. *N-Wasp*$^{\Delta/\Delta}$ pancreata showed no abnormalities (Fig. S5B) and FPE levels in *N-Wasp*$^{\Delta/\Delta}$ explants were unaffected (Fig. S5C). Three-months-old *Kras*^{G12D}*;N-Wasp*$^{\Delta/\Delta}$ mice, which did not express N-WASP (Fig. 5D), presented large areas with acinar tissue, fatty metaplasia and infiltrating cells (Fig. S5D). Notably, *Kras*^{G12D}*;N-Wasp*$^{\Delta/\Delta}$ mice showed significantly less ADM lesions compared to *Kras*^{G12D} mice and developed no PanIN lesions (Figs. 5E-G, S5E). Acinar cells did not express P-ERK in the pancreas of neither *Kras*^{G12D} nor *Kras*^{G12D}*;N-Wasp*$^{\Delta/\Delta}$ mice at the age of four 4 weeks (Fig. S5I). At the age of three months, *Kras*^{G12D} mice showed diffuse P-ERK expression in ADM land PanIN lesions and acinar cells, while *Kras*^{G12D}*; N-Wasp*$^{\Delta/\Delta}$ mice did not express P-ERK in the morphologically appearing normal acinar cells (Fig. 5H).

In order to confirm the requirement of *N-Wasp* for ADM, we isolated acinar explants from 4 weeks old *Kras*^{G12D}*;N-Wasp*$^{\Delta/\Delta}$ mice which did not express N-WASP (Supp. Fig. 5F). *Kras*^{G12D}*;N-Wasp*$^{\Delta/\Delta}$ explants did not develop ADM while maintaining an acinar phenotype (Fig. 5I-J). We next determined fluid-phase endocytosis rates in *Kras*^{G12D}*;N-Wasp*$^{\Delta/\Delta}$ explants that were significantly reduced (Fig. 5K), supporting the requirement of FPE for ADM *in vivo*. In agreement with these results, a cell line generated from a *Kras*^{G12D}*;N-Wasp*$^{\Delta/\Delta}$ mouse and lacking N-WASP expression had reduced FPE compared to control cells (Fig. S5G–H). Thus, we provide *in vivo* genetic evidence that N-WASP is required for KRas-driven ADM development and sustained FPE.

4. Discussion

Mutant KRas is involved in the development of many malignancies and is the sole oncogenic driver in PDAC (Eser et al., 2014; Pylayeva-Gupta et al., 2011). Signal transduction of the KRas pathway can take place both at the plasma membrane and in the endosomal compartment; however, the relevance of the latter in a physiological context is largely unknown (Fehrenbacher et al., 2009; Mor and Philips, 2006). Oncogenic KRas drives pancreatic acinar cells to develop PDAC through a process of ADM in cooperation with EGFR signaling (Ardito et al., 2012; Navas et al., 2012). KRas^{G12D} increases the levels of mitochondrial reactive oxygen species to increase *EGFR* transcription and also leads to increased macropinocytosis in transformed cells (Commisso et al., 2013; Liou et al., 2016). However; whether KRas requires the endocytic compartment for preneoplastic development is largely unknown.

Here, we used three-dimensional cultures of acinar epithelial explants to investigate the role of fluid-phase endocytosis in ADM development. The benefits of this method are: (i) explants expressing oncogenic KRas are not yet transformed; (ii) they develop ductal structures over time without proliferation; (iii) they are cultivated in three-dimensional collagen matrices, mimicking the *in vivo* cell morphological changes during ADM. We show that acinar exocrine tissue under physiological conditions has low fluid-phase endocytosis, which increases upon activation of KRas^{G12D} and requires expression of EGFR. An increase in FPE levels of acinar explants in response to changes in variations in plasma membrane tension is sufficient to induce ADM independently of EGFR expression and *vice versa* pharmacological inhibition of endocytosis impairs ADM *in vitro*. Several limitations need consideration: (i) we cannot exclude the involvement of FPE-independent pathways or mechanisms after the hypoosmotic treatment and/or by the mechanical strain applied; (ii) the pharmacological approaches are not specific for FPE, but also affect other pathways such as the PI3K and lysosomal pathways; (iii) the genetic deletion of *Rac1* and *N-Wasp* may involve also pathways other than FPE. Nevertheless, our data suggest that the requirement of EGFR for KRas^{G12D}-induced ADM may be through regulation of FPE since also the PI3K pathway is connected to the endosomal function (Simonsen et al., 1998).

Fluid-phase endocytosis involves several endocytic mechanisms that are characterized by fluids as a cargo (reviewed in (Doherty and McMahon, 2009)). While we did not characterize further the mechanism regulating FPE involved during ADM, we show here that the central regulatory role of RAC1 in ADM formation may be in part through actin-dependent regulation of fluid-phase endocytosis.

Mechanistically, we hypothesize that RAB5 + early endosomes may act as a scaffold for ERK activation. The increase in ERK phosphorylation goes along with the increase of FPE and conversely, inhibition of MEK/ERK activation does not affect the increase of FPE but inhibits ADM following perturbations in the plasma membrane supporting this hypothesis; additionally, IQGAP1, which has been shown to be required for ERK activation in KRas-driven tumors, interacts with early endosomes and is potentially involved in this pathway (Jacquemet and Humphries, 2013;

Fig. 2. FPE increases while ADM occurs and is *Rac1* dependent but *Egfr*-dependent. (A) Acinar explants were starved overnight, then compounds were added for 10 min and a HRP assay was performed. Mean ± SD. Two tailed *t*-test. (B, C) *Kras*^{G12D} acinar explants were isolated from at least three mice and seeded in collagen. Monensin or wortmannin were added to the medium and ADM was quantified at day 3. In the scatter dot plots each dot represents the number of structures/optical field. Red lines: mean ± SD. Mann-Whitney test. (D) Western blot of *Kras*^{G12D} acinar explants treated with the indicated compounds for 10 min. (E, F) Acinar explants were starved overnight and treated the next day with refametinib and EGF (25 ng/ml) for the indicated time points. (E) Western blot and (F) HRP uptake assay ($N = 4$ mice). Mean ± SD. Mann-Whitney test. (G) Acinar explants were starved overnight. The next day CytD was added together with EGF and a HRP uptake assay was performed. Mean ± SD, two-tailed *t*-test. (H) Acinar explants were isolated from mice of the indicated genotypes (2 mice per group) and were then starved overnight. The next day the explants were treated with EGF (25 ng/ml) for 10 min. An HRP uptake assay was performed and normalized to the HRP uptake of untreated acini. Mean ± SD, two-tailed *t*-test. (I) Acinar explants were isolated from mice of the indicated genotypes and were then starved overnight. Wild type explants treated with EGF were used as a control. The next day an HRP-assay was performed in triplicates. The increase in FPE of *Kras*^{G12D} and *Kras*^{G12D}*;Rac1*$^{\Delta/\Delta}$ explants compared to the control is shown. Mean ± SD, two-tailed *t*-test. (J) Acinar explants were isolated from mice of the indicated genotypes and a dextran endocytic assay was performed. Representative total Z-projections. Scale bars = 50 μm. (K) Quantification of the endocytic assay as in (L). Red lines: mean ± SD, Mann-Whitney test.

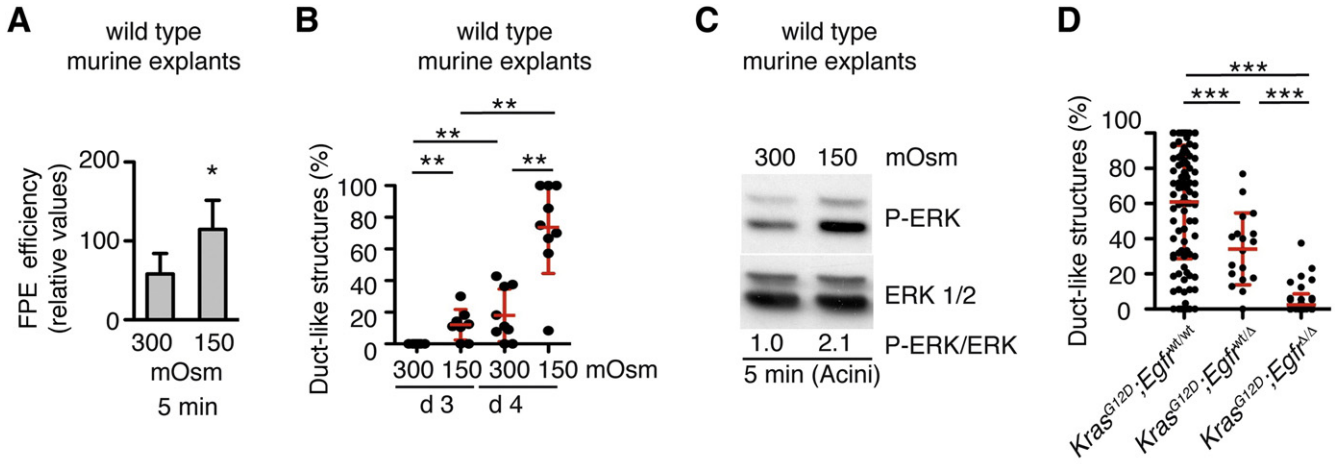
A
wild type murine explants
FPE efficiency (relative values)
300 150 mOsm
5 min
B
wild type murine explants
Duct-like structures (%)
300 150 300 150 mOsm
d 3 d 4
C
wild type murine explants
300 150 mOsm
P-ERK
ERK 1/2
1.0 2.1 P-ERK/ERK
5 min (Acini)
D
Duct-like structures (%)
KrasG12D;EgfrWt/Wt
KrasG12D;EgfrWt/Δ
KrasG12D;EgfrΔ/Δ

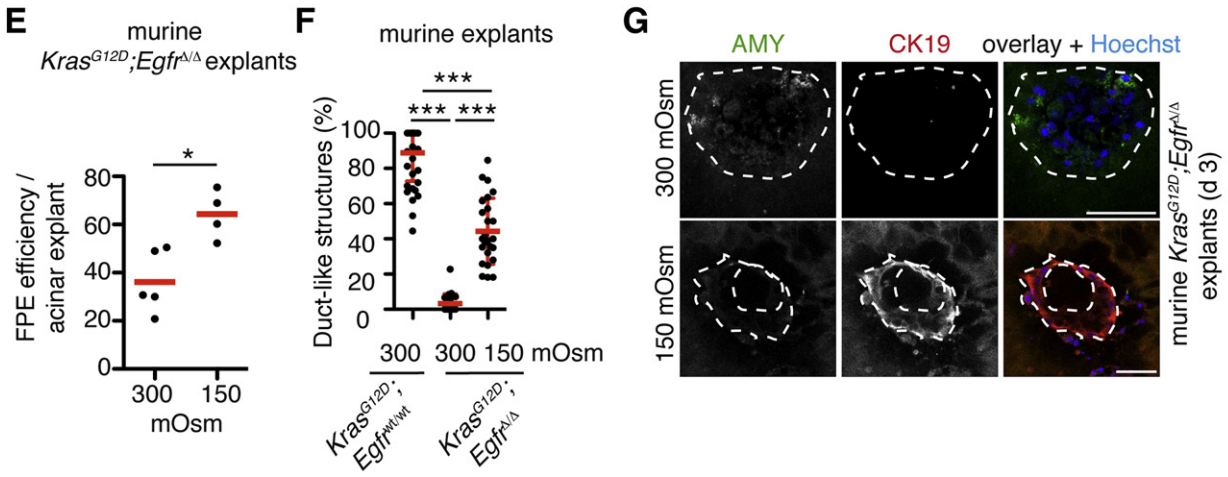
E
murine KrasG12D;EgfrΔ/Δ explants
FPE efficiency / acinar explant
300 150 mOsm
F
murine explants
Duct-like structures (%)
300 300 150 mOsm
KrasG12D; EgfrWt/Wt
KrasG12D; EgfrΔ/Δ
G
AMY
CK19
overlay + Hoechst
300 mOsm
150 mOsm
murine KrasG12D;EgfrΔ/Δ explants (d 3)

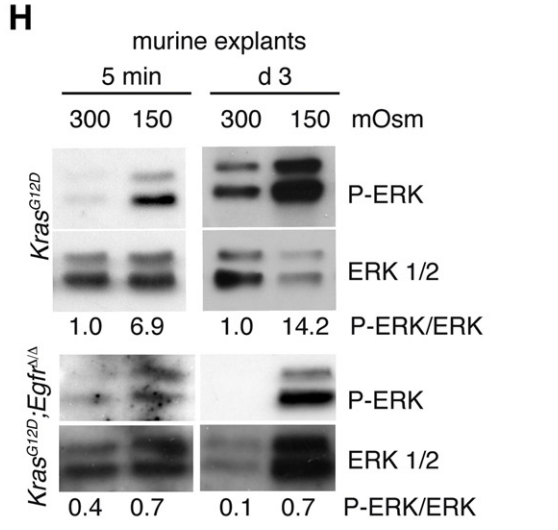
H
murine explants
5 min
d 3
300 150 300 150 mOsm
KrasG12D
P-ERK
ERK 1/2
1.0 6.9 1.0 14.2 P-ERK/ERK
KrasG12D;EgfrΔ/Δ
P-ERK
ERK 1/2
0.4 0.7 0.1 0.7 P-ERK/ERK

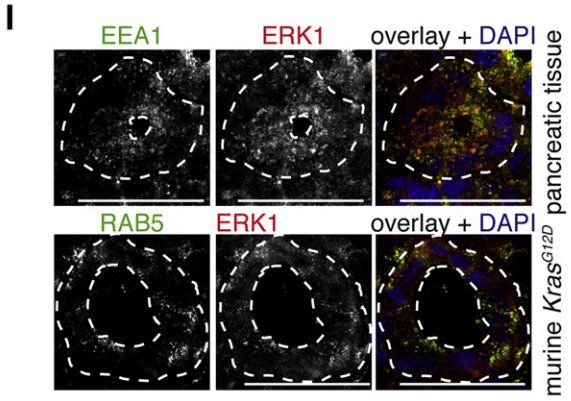
I
EEA1
ERK1
overlay + DAPI
RAB5
ERK1
overlay + DAPI
murine KrasG12D pancreatic tissue

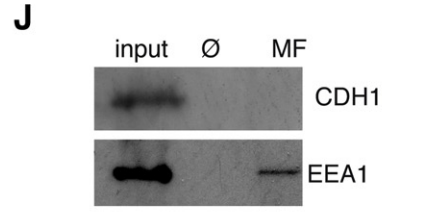
J
input Ø MF
CDH1
EEA1
murine KrasG12D pancreatic tissue

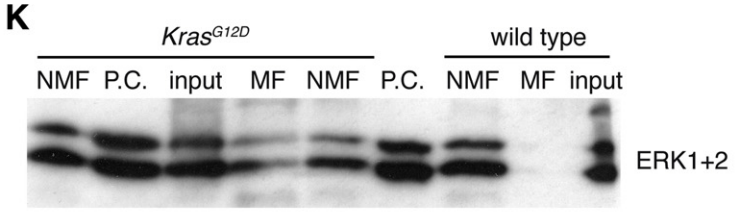
K
KrasG12D
wild type
NMF P.C. input MF NMF P.C. NMF MF input
ERK1+2
murine pancreatic tissue

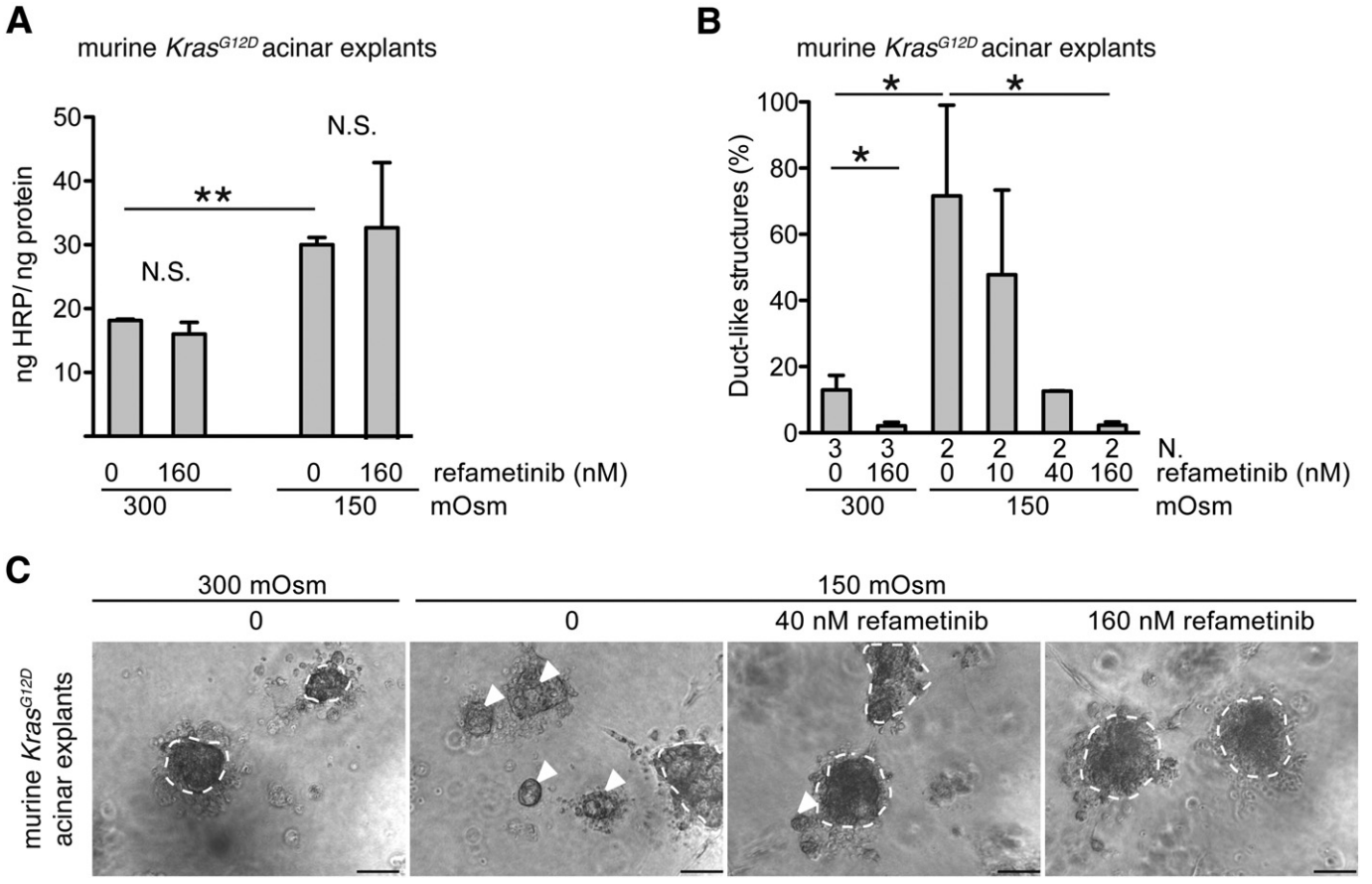

Fig. 4. MEK inhibition of hypoosmolar-induced ADM. In all panels $Kras^{G12D}$ acinar explants were isolated and starved overnight. The next day explants were incubated with hypoosmotic (150 mOsm) medium for 5 min and then refametinib was added at the indicated concentrations. (A) HRP assay from two mice was performed immediately after the 5 min hypoosmotic treatment. Mean ± SD, two-tailed *t*-test. (B) Acinar explants were seeded in collagen and ADM was quantified at day 4. N = number of mice. Mean ± SD, two-tailed *t*-test. (C) Representative bright field images of acinar explants described in B. Dashed lines highlight acinar cell clusters, arrowheads: duct-like structures. Scale bars = 50 μm.

Jameson et al., 2013). This working model is also supported by the observation that part of the intracellular ERK pool associates with the RAB5 + endosomal compartment in ADM lesions. Notably, IQGAP1 is known to interact with the actin-nucleation factor N-WASP (Takenawa and Miki, 2001), which is intimately connected to EGFR protein expression because it regulates its internalization (Benesch et al., 2005) and expression of both *EGFR* and *WASL* positively correlates in human expression data as shown here. Here we show that N-WASP is upregulated during early pancreatic carcinogenesis. Conditional deletion of *N-Wasp* in the *KRas-*^{G12D} model impaired development of preneoplastic lesions by reducing FPE in acinar tissue, thus supporting the *in vivo* relevance of our findings and highlighting the causative role of N-WASP-dependent FPE for the development of precancerous lesions.

In summary, oncogenic KRas-induced increase in fluid-phase endocytosis has a key role during cellular transdifferentiation in pancreatic acinar cells. This result supports emerging evidence for endocytosis playing a crucial role in regulating the signaling output of the cells (Fehrenbacher et al., 2009; Murphy et al., 2009; Scita and Di Fiore, 2010; Sorkin and von Zastrow, 2009). More insights into the crucial regulatory function of the endocytic compartment in PDAC development will help understand the complex role of KRas-dependent signaling with the potential for novel targeting approaches.

We confirm that there are no known conflicts of interest associated with this publication and there has been no significant financial support for this work that could have influenced its outcome.

Supplementary data to this article can be found online at http://dx.doi.org/10.1016/j.ebiom.2016.12.013.

Author Contributions

C.L.M and J.T.S. designed research; C.L.M., K.A. and A.H.S performed research; I.H. performed *in vivo* experiments; S.B and T.B performed some experiments; C.L.M. and K.A. analyzed data; C.L.M, R.M.S and J.T.S. discussed the data; C.L.M, R.M.S. and J.T.S. contributed with funding and resources; C.L.M and J.T.S. wrote the paper.

Fig. 3. Changes in plasma membrane tension increase FPE and induce ADM independently of *Egfr*. (A) Acinar explants from three mice were starved overnight and incubated for 5 min in 0.1% FCS media of different osmolarity. Afterwards a FPE assay was performed. Mean ± SD, two-tailed *t*-test. (B) Explants from three mice treated like in (A) were plated in collagen matrix. ADM was quantified at day 3. Mann-Whitney test. (C) Acinar explants were treated like in (A). Total protein lysates were extracted immediately after the hypoosmolar treatment and analyzed by Western blot. (D) Acinar explants were isolated from mice (up to 14 mice per genotype) and ADM was quantified at day 3. Each dot represents the number of structures/optical field. Red lines: mean ± SD. Mann-Whitney test. (E) Dextran uptake assay of $Kras^{G12D}$;$Egfr^{\Delta/\Delta}$ acinar explants treated with hypoosmolar media for 5 min. Red lines: mean; Mann-Whitney test. (F) Explants from 4 mice were treated like in (E) and were then plated in collagen matrix. ADM was quantified at day 3. Each dot represents the number of structures/optical field. Red lines: mean ± SD. Mann-Whitney test. (G) Immunofluorescence staining showing the rescued phenotype of $Kras^{G12D}$;$Egfr^{\Delta/\Delta}$ explants after hypoosmotic treatment. Scale bars = 50 μm. (H) Western blot of $Kras^{G12D}$;$Egfr^{\Delta/\Delta}$ and $Kras^{G12D}$ acinar explants incubated 5 min with hypoosmotic medium and analyzed at the indicated time points. (I) Immunofluorescence staining for ERK1 and the markers for early endosomes (EEA1 and RAB5) in $Kras^{G12D}$ pancreatic tissue. Dashed lines: ADM lesions. Images were taken by sequential scan of each wavelength to avoid bleed-through. Scale bars = 10 μm. (J,K) Western blots of the RAB5 + eluted magnetic fraction (MF) immunoisolated from whole pancreatic tissue (M = marker; P.C. = positive control, whole protein lysate from murine pancreatic cell line).

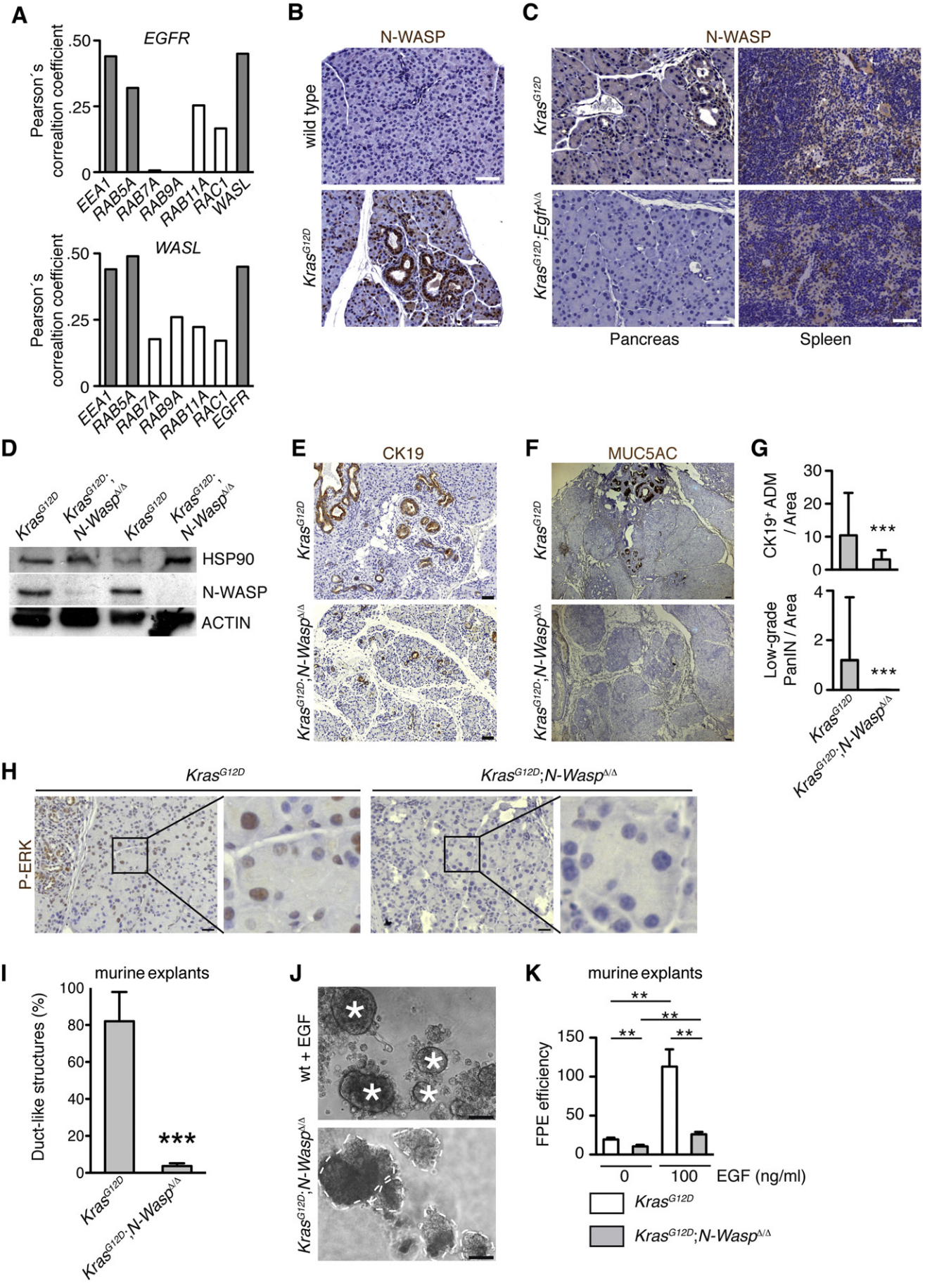
A
EGFR
Pearson´s correaltion coefficient
.50
.25
0
EEA1
RAB5A
RAB7A
RAB9A
RAB11A
RAC1
WASL
WASL
Pearson´s correaltion coefficient
.50
.25
0
EEA1
RAB5A
RAB7A
RAB9A
RAB11A
RAC1
EGFR
B
N-WASP
wild type
KrasG12D
C
N-WASP
KrasG12D
KrasG12D;EgfrΔ/Δ
Pancreas
Spleen
D
KrasG12D
KrasG12D; N-WaspΔ/Δ
KrasG12D
KrasG12D; N-WaspΔ/Δ
HSP90
N-WASP
ACTIN
E
CK19
KrasG12D
KrasG12D;N-WaspΔ/Δ
F
MUC5AC
KrasG12D
KrasG12D;N-WaspΔ/Δ
G
CK19+ ADM / Area
30
20
10
0
***
Low-grade PanIN / Area
4
2
0
***
KrasG12D
KrasG12D;N-WaspΔ/Δ
H
KrasG12D
KrasG12D;N-WaspΔ/Δ
P-ERK
I
murine explants
Duct-like structures (%)
100
80
60
40
20
0
***
KrasG12D
KrasG12D;N-WaspΔ/Δ
J
wt + EGF
KrasG12D;N-WaspΔ/Δ
K
murine explants
**
**
**
**
FPE efficiency
150
100
50
0
0
100
EGF (ng/ml)
KrasG12D
KrasG12D;N-WaspΔ/Δ

Acknowledgments

We would like to thank A. Berns, D. Tuveson, T. Jacks, M. Sibilia and C. Brakebusch for providing transgenic animals and J. Kleeff, M. Erkan and G. Ceyhan for providing human samples. We thank M. Schiemann for use of the Leica confocal microscope and R. Braren for infrastructural support. We thank U. Ehmer and H. Einwächter for discussion of results.

The results published here are in part based upon data generated by the TCGA Research Network: http://cancergenome.nih.gov/.

This project was supported by the Deutsche Forschungsgemeinschaft (LU1943/1 to C.L.M and SI1549/2-1 to J.T.S.), the Wilhelm Sander-Stiftung (2010.021.1 to J.T.S.), by the Deutsche Krebshilfe (#109992 to J.T.S.) and by the German Cancer Consortium (DKTK, to R.M.S. and J.T.S.).

References

Aichler, M., Seiler, C., Tost, M., Siveke, J., Mazur, P.K., Da Silva-Buttkus, P., Bartsch, D.K., Langer, P., Chiblak, S., Durr, A., et al., 2012. Origin of pancreatic ductal adenocarcinoma from atypical flat lesions: a comparative study in transgenic mice and human tissues. J. Pathol. 226, 723–734.

Almoguera, C., Shibata, D., Forrester, K., Martin, J., Arnheim, N., Perucho, M., 1988. Most human carcinomas of the exocrine pancreas contain mutant c-K-ras genes. Cell 53, 549–554.

Apodaca, G., 2002. Modulation of membrane traffic by mechanical stimuli. Am. J. Physiol. Ren. Physiol. 282, F179–F190.

Ardito, C.M., Gruner, B.M., Takeuchi, K.K., Lubeseder-Martellato, C., Teichmann, N., Mazur, P.K., Delgiorno, K.E., Carpenter, E.S., Halbrook, C.J., Hall, J.C., et al., 2012. EGF receptor is required for KRAS-induced pancreatic tumorigenesis. Cancer Cell 22, 304–317.

Benesch, S., Polo, S., Lai, F.P., Anderson, K.I., Stradal, T.E., Wehland, J., Rottner, K., 2005. N-WASP deficiency impairs EGF internalization and actin assembly at clathrin-coated pits. J. Cell Sci. 118, 3103–3115.

Cerami, E., Gao, J., Dogrusoz, U., Gross, B.E., Sumer, S.O., Aksoy, B.A., Jacobsen, A., Byrne, C.J., Heuer, M.L., Larsson, E., et al., 2012. The cBio cancer genomics portal: an open platform for exploring multidimensional cancer genomics data. Cancer Discov. 2, 401–404.

Commisso, C., Davidson, S.M., Soydaner-Azeloglu, R.G., Parker, S.J., Kamphorst, J.J., Hackett, S., Grabocka, E., Nofal, M., Drebin, J.A., Thompson, C.B., et al., 2013. Macropinocytosis of protein is an amino acid supply route in Ras-transformed cells. Nature 497, 633–637.

Doherty, G.J., McMahon, H.T., 2009. Mechanisms of endocytosis. Annu. Rev. Biochem. 78, 857–902.

Eser, S., Reiff, N., Messer, M., Seidler, B., Gottschalk, K., Dobler, M., Hieber, M., Arbeiter, A., Klein, S., Kong, B., et al., 2013. Selective requirement of PI3K/PDK1 signaling for Kras oncogene-driven pancreatic cell plasticity and cancer. Cancer Cell 23, 406–420.

Eser, S., Schnieke, A., Schneider, G., Saur, D., 2014. Oncogenic KRAS signalling in pancreatic cancer. Br. J. Cancer.

Fehrenbacher, N., Bar-Sagi, D., Philips, M., 2009. Ras/MAPK signaling from endomembranes. Mol. Oncol. 3, 297–307.

Gao, J., Aksoy, B.A., Dogrusoz, U., Dresdner, G., Gross, B., Sumer, S.O., Sun, Y., Jacobsen, A., Sinha, R., Larsson, E., et al., 2013. Integrative analysis of complex cancer genomics and clinical profiles using the cBioPortal. Sci. Signal. 6, pl1.

Grant, B.D., Donaldson, J.G., 2009. Pathways and mechanisms of endocytic recycling. Nat. Rev. Mol. Cell Biol. 10, 597–608.

Hanahan, D., Weinberg, R.A., 2011. Hallmarks of cancer: the next generation. Cell 144, 646–674.

Heid, I., Lubeseder-Martellato, C., Sipos, B., Mazur, P.K., Lesina, M., Schmid, R.M., Siveke, J.T., 2011. Early requirement of Rac1 in a mouse model of pancreatic cancer. Gastroenterology 141, 719–730 (730 e711-717).

Hingorani, S.R., Petricoin, E.F., Maitra, A., Rajapakse, V., King, C., Jacobetz, M.A., Ross, S., Conrads, T.P., Veenstra, T.D., Hitt, B.A., et al., 2003. Preinvasive and invasive ductal pancreatic cancer and its early detection in the mouse. Cancer Cell 4, 437–450.

Hruban, R.H., Iacobuzio-Donahue, C., Wilentz, R.E., Goggins, M., Kern, S.E., 2001. Molecular pathology of pancreatic cancer. Cancer J. 7, 251–258.

Iverson, C., Larson, G., Lai, C., Yeh, L.T., Dadson, C., Weingarten, P., Appleby, T., Vo, T., Maderna, A., Vernier, J.M., et al., 2009. RDEA119/BAY 869766: a potent, selective, allosteric inhibitor of MEK1/2 for the treatment of cancer. Cancer Res. 69, 6839–6847.

Jacquemet, G., Humphries, M.J., 2013. IQGAP1 is a key node within the small GTPase network. Small GTPases 4, 199–207.

Jameson, K.L., Mazur, P.K., Zehnder, A.M., Zhang, J., Zarnegar, B., Sage, J., Khavari, P.A., 2013. IQGAP1 scaffold-kinase interaction blockade selectively targets RAS-MAP kinase-driven tumors. Nat. Med. 19, 626–630.

Joffre, C., Barrow, R., Menard, L., Calleja, V., Hart, I.R., Kermorgant, S., 2011. A direct role for Met endocytosis in tumorigenesis. Nat. Cell Biol. 13, 827–837.

Li, G., D'Souza-Schorey, C., Barbieri, M.A., Roberts, R.L., Klippel, A., Williams, L.T., Stahl, P.D., 1995. Evidence for phosphatidylinositol 3-kinase as a regulator of endocytosis via activation of Rab5. Proc. Natl. Acad. Sci. U. S. A. 92, 10207–10211.

Liou, G.Y., Doppler, H., DelGiorno, K.E., Zhang, L., Leitges, M., Crawford, H.C., Murphy, M.P., Storz, P., 2016. Mutant KRas-induced mitochondrial oxidative stress in acinar cells upregulates EGFR signaling to drive formation of pancreatic precancerous lesions. Cell Rep. 14, 2325–2336.

Lommel, S., Benesch, S., Rottner, K., Franz, T., Wehland, J., Kuhn, R., 2001. Actin pedestal formation by enteropathogenic *Escherichia coli* and intracellular motility of Shigella flexneri are abolished in N-WASP-defective cells. EMBO Rep. 2, 850–857.

Lubeseder-Martellato, C., 2013. Isolation, culture and differentiation of primary acinar epithelial explants from adult murine pancreas. In BioProtocol.

Means, A.L., Meszoely, I.M., Suzuki, K., Miyamoto, Y., Rustgi, A.K., Coffey Jr., R.J., Wright, C.V., Stoffers, D.A., Leach, S.D., 2005. Pancreatic epithelial plasticity mediated by acinar cell transdifferentiation and generation of nestin-positive intermediates. Development 132, 3767–3776.

Mor, A., Philips, M.R., 2006. Compartmentalized Ras/MAPK signaling. Annu. Rev. Immunol. 24, 771–800.

Mosesson, Y., Mills, G.B., Yarden, Y., 2008. Derailed endocytosis: an emerging feature of cancer. Nat. Rev. Cancer 8, 835–850.

Murphy, J.E., Padilla, B.E., Hasdemir, B., Cottrell, G.S., Bunnett, N.W., 2009. Endosomes: a legitimate platform for the signaling train. Proc. Natl. Acad. Sci. U. S. A. 106, 17615–17622.

Navas, C., Hernandez-Porras, I., Schuhmacher, A.J., Sibilia, M., Guerra, C., Barbacid, M., 2012. EGF receptor signaling is essential for k-ras oncogene-driven pancreatic ductal adenocarcinoma. Cancer Cell 22, 318–330.

Oda, K., Matsuoka, Y., Funahashi, A., Kitano, H., 2005. A comprehensive pathway map of epidermal growth factor receptor signaling. Mol. Syst. Biol. 1 (2005), 0010.

Pylayeva-Gupta, Y., Grabocka, E., Bar-Sagi, D., 2011. RAS oncogenes: weaving a tumorigenic web. Nat. Rev. Cancer 11, 761–774.

Scita, G., Di Fiore, P.P., 2010. The endocytic matrix. Nature 463, 464–473.

Simonsen, A., Lippe, R., Christoforidis, S., Gaullier, J.M., Brech, A., Callaghan, J., Toh, B.H., Murphy, C., Zerial, M., Stenmark, H., 1998. EEA1 links PI(3)K function to Rab5 regulation of endosome fusion. Nature 394, 494–498.

Sorkin, A., von Zastrow, M., 2009. Endocytosis and signalling: intertwining molecular networks. Nat. Rev. Mol. Cell Biol. 10, 609–622.

Stein, B.S., Bensch, K.G., Sussman, H.H., 1984. Complete inhibition of transferrin recycling by monensin in K562 cells. J. Biol. Chem. 259, 14762–14772.

Stenmark, H., 2009. Rab GTPases as coordinators of vesicle traffic. Nat. Rev. Mol. Cell Biol. 10, 513–525.

Takenawa, T., Miki, H., 2001. WASP and WAVE family proteins: key molecules for rapid rearrangement of cortical actin filaments and cell movement. J. Cell Sci. 114, 1801–1809.

Warren, C.M., Landgraf, R., 2006. Signaling through ERBB receptors: multiple layers of diversity and control. Cell. Signal. 18, 923–933.

Fig. 5. Oncogenic KRas-driven preneoplastic development requires N-WASP. (A) Data were retrieved from PDAC samples from the cBioPortal (TGCA provisional, $N = 145$) and correlation between mRNA expression of the indicated gene pairs was analyzed using the "Plot" tool. (B) Immunohistological staining for N-WASP in pancreatic tissue of 4-weeks-old mice of the indicated genotypes. (C) Immunohistological staining for N-WASP in pancreatic tissue from mice of the indicated genotypes. Spleens of the same mice were used as internal positive control. (D) Western blot of pancreatic tissue of three-month-old mice as indicated. (E, F) Immunohistological staining of pancreatic tissue for the ductal marker cytokeratin 19 (CK19) and the PanIN marker mucin 5 AC (MUC5AC) in three-month-old mice. (G) Morphometric quantification of preneolastic lesions in mice of the indicated genotypes. $Kras^{G12D}$ ($N = 4$, 323 optical fields) and $Kras^{G12D}$;$N\text{-}Wasp^{\Delta/\Delta}$ ($N = 3$, 186 optical fields). Mean ± SD, Mann-Whitney test. (H) Immunohistological staining for P-ERK in pancreatic tissue from three-month-old mice of the indicated genotypes. The insert highlights pancreatic acini. (I) Acinar explants from mice with the indicated genotypes ($Kras^{G12D}$ $N = 5$ and $Kras^{G12D}$;$N\text{-}Wasp^{\Delta/\Delta}$ $N = 3$) were cultured in collagen matrix. ADM was quantified at day 3. Mean and SD are shown, 2-tailed *t*-test. (J) Bright field images of explants described in (I). Dashed lines highlight acinar cell clusters. Asterisks mark the ducts. (K) Acinar tissue was isolated from littermate mice and acinar explants were starved overnight, then a FPE assay was performed. Mean ± SD. All scale bars = 50 μm.